Optimal Operation of Integrated Water–Power Systems Under Contingencies

Mohannad Alhazmi, *Student Member, IEEE*, Payman Dehghanian, *Senior Member, IEEE*, Mostafa Nazemi, *Student Member, IEEE*, Fei Wang, *Senior Member, IEEE*, and Abdullah Alfadda

***Abstract*—With the sharply growing complexity and rapid deployment of smart technologies in our modern society, risk-aware management and coordination in day-to-day operation of the interlinked critical infrastructures is urgently needed. In particular, the interconnected water and power systems (WaPS) are in need of joint and cooperative operation to maximize the economic benefits during normal operating conditions and resilience services during emergencies. While contingency analysis is used to assist the system operators in gaining knowledge of the system's static security, such understanding is more challenging to achieve in the case of integrated WaPS. This article proposes a novel optimization model for under-emergency operation of the integrated WaPS, considering contingencies in both networks. In order to ensure the delivery of water demand, the proposed formulation considers the hydraulic constraints of the water networks, which is naturally a nonlinear model. The proposed nonlinear model is approximated using a piece-wise linearization approach to convert the optimization model into a mixed-integer linear programming formulation. The proposed analytics are applied to a modified IEEE 24-bus reliability test system that is jointly operated with two and three commercial-scale water networks. The proposed model is evaluated using various disaster severity levels (i.e., $N-k$ contingency scenarios) and verify the promising performance of the proposed integrated WaPS model when facing failures and threatening high impact low probability emergencies.**

***Index Terms*—Contingency analysis, dc optimal power flow (DCOPF), emergency response, interdependent networks, water and power systems (WaPS), water–energy nexus (WEN).**

Manuscript received July 31, 2021; revised November 13, 2021 and January 28, 2022; accepted March 27, 2022. Date of publication April 19, 2022; date of current version July 19, 2022. Paper 2021-PSEC-0971.R2, presented at the 2021 IEEE Industry Applications Society Annual Meeting, Vancouver, BC Canada, Oct. 10–14, and approved for publication in the IEEE TRANSACTIONS ON INDUSTRY APPLICATIONS by the Power Systems Engineering Committee of the IEEE Industry Applications Society. This work was supported in part by the U.S. National Science Foundation (NSF) under Grant CNS-1951847. *(Corresponding author: Payman Dehghanian.)*

Mohannad Alhazmi is with the Department of Electrical and Computer Engineering, George Washington University, Washington, DC 20052 USA, and also with the Department of Electrical Engineering, College of Engineering, King Saud University, Riyadh 11421, Saudi Arabia (e-mail: alhazmi@gwu.edu).

Payman Dehghanian and Mostafa Nazemi are with the Department of Electrical and Computer Engineering, George Washington University, Washington, DC 20052 USA (e-mail: payman@gwu.edu; mostafa_nazemi@gwu.edu).

Fei Wang is with the Electrical Engineering Department, North China Electric Power University, Baoding 071003, China (e-mail: feiwang@ncepu.edu.cn).

Abdullah Alfadda is with the Center of Excellence for Telecommunication Applications, King Abdulaziz City for Science and Technology, Riyadh 12354, Saudi Arabia (e-mail: aalfadda@kacst.edu.sa).

Color versions of one or more figures in this article are available at https://doi.org/10.1109/TIA.2022.3167661.

Digital Object Identifier 10.1109/TIA.2022.3167661

NOMENCLATURE

A. *Sets*

$g \in NG$	Set of system generating units.
$t \in NT$	Set of time intervals.
$n \in B$	Set of system buses.
$k \in L$	Set of system transmission lines.
$r \in \mathcal{R}$	Set of water system reservoirs.
p $\in \mathcal{P}$	Set of water system pumps.
s $\in \mathcal{S}$	Set of water system pipes.

B. *Variables and Functions*

P_t^{sh}	The shedding amount of load at time t.
Q_t	Water flow rate at time t.
R_t^r	Vector of reservoirs' water inflow rate for each reservoir r at time t.
Q_t^j	Water flow rate through pipe j at time t.
Q_t^p	Water flow rate through pump p at time t.
H_t	Pressure heads at time t.
$H_{n,t}^j$	Pressure heads associated with pipe j and node n at time t.
$H_{n,t}^p$	Pressure heads associated with pump p and node n at time t.
H_t^r	Pressure heads associated with reservoir r at time t.
Sign(.)	Sign function.
ΔE_t	The difference of tanks' inflow/outflow rate at time t.
T_t^{in}	Vector of water inflow to tanks at time t.
T_t^{out}	Vector of water outflow to tanks at time t.
V_t	Volume of stored water in tanks at time t.
W_t	Pumps' speed at time t.
P_t^p	Power consumption for pump p at time t.
$P_{b,t}^{p,\text{adj}}$	Vector of water electricity consumption in bus b at time t.
$X_t^{i,j}$	Continuous decision variable for pressure head breakpoint i associated with pipe j at time t.
$X_t^{u,m,p}$	Continuous decision variable for pressure head breakpoint u associated with pump p at time t.
$P_{g,t}$	Expected power output of generating unit g at time t.
$P_{k(nm),t}$	Power flow through transmission line k (connecting bus n to m) at time t.
$P_{dn,t}$	Total power-water demand at time t (MW).
$\theta_{i,t}$	Voltage angle for bus i at time t.

C. Binary Variables

$Y_t^{i,j}$	Binary variable for pressure head breakpoint i associated with pipe j at time t.
$H_{i,m,p,t}^{\text{Upper}}$	Binary variable for the upper triangle in the rectangle at time t.
$H_{i,m,p,t}^{\text{Lower}}$	Binary variable for the lower triangle in the rectangle at time t.
$\phi_{g,t}$	Binary variable for the connection status of generator g at time t (1 if it is available, 0 otherwise).
$\nu_{k,t}$	Binary variable for the connection status of power line k at time t (1 if it is online, 0 otherwise).
τ_t^p	Binary variable for the connection status of pump stations p at time t (1 if it is online, 0 otherwise).

D. Parameters

$P_{d,t}$	Total electricity demand at time t.
$\overline{P_{\text{dn}}}, \underline{P_{\text{dn}}}$	Maximum/Minimum electricity demand.
x_k	Reactance of transmission line k.
$P_k^{\max}$	Maximum power flow limit of line k.
$P_g^{\max}$	Maximum capacity limit of generating unit g.
$P_g^{\min}$	Minimum capacity limit of generating unit g.
D_t	Vector of water demand (m^3/s) at time t.
$\hat{H}$	Reservoirs' geographical height.
$V_{\min}$	Tanks' minimum volume.
$V_{\max}$	Tanks' Maximum volume.
$\underline{\Delta E}$	Minimum charging/discharging difference for tanks.
$\overline{\Delta E}$	Maximum charging/discharging difference for tanks.
r_p	Pipe parameter.
$H_{\min}$	Minimum nodal pressure heads.
$H_{\max}$	Maximum nodal pressure heads.
$Q_{\max/\min}$	Maximum/Minimum water flow rate to the network.
$P_{\max/\min}^p$	Maximum/Minimum power consumption for pump p.
q_i^p	Water flow rate of breakpoint i for pump p.
q_i^j	Water flow rate of breakpoint i for pipe j.
c_t^{sh}	The price of shedding load at time t (\$/MW).
$c_{r,t}$	Vector of reservoirs' water price at time t.
$c_{g,t}$	linear cost coefficients of generating unit g at time t (\$/MW).
w_i^p	Speed breakpoint i for pump p.
$a_{1,2,3}, z_{1,2}$	Performance parameters for pumps.
$\mathcal{C}$	Incidence matrix of pumps' location.

I. Introduction

POWER and water networks are known among the most critical interconnected infrastructures due to their crucial role in human life and our modern society. Water networks are considered the most energy-intensive shareholder of the total electricity demand [1]. Approximately 4% of the electricity consumption in the United States is utilized by water networks around the country [2]. Drinking water and wastewater account for around 40% of the consumed energy for local governments [3]. Furthermore, water networks in California absorb around 20% of the total electricity consumed [4]. Therefore, there is an urgent need to improve the water networks' operation reliability and resiliency, i.e., water treatment, water purification, cooling, wastewater, etc., as the demanded electricity associated with water facilities is projected to increase due to the sharp rise in the population and use in industry applications.

In the traditional practice, water and power systems (WaPS) have been designed and planned as two separate and uncoupled systems, while in reality, the operation of both systems is jointly interdependent [5]. Power system operators are in need of water for refining fuels and generating electricity, while on the other hand, water facilities require electricity in order to operate normally. Further, the operation of mutually interdependent power and water systems is more critical and challenging in the case of limited availability of resources or failures in either network. If a shortage in delivering the demanded electricity is realized, water networks may not be supplied with sufficient energy required for pumping the water through pipelines, resulting in a failure in both networks. This interrelationship ecosystem of water and power is commonly known as water–energy nexus (WEN) [6]–[8].

Predominantly, the WEN has been investigated in the literature regarding policy, regulatory challenges, and its connections to economic growth and climate change [9]–[11]. Kao *et al.*[12] studied the impact of climate change on water reservoir management and hydropower plant operation. A literature review on water distribution network optimization with respect to WEN is studied in [13]. A physics-based approach for modeling WEN to optimize the structure of water, wastewater, and power systems is studied in [14]. WEN linkage analysis is investigated in [15] to illustrate the effect of considering the interaction of coupled WaPS on various economic sectors. Optimal dispatch of WaPS and its impact on battery storage is studied in [16]. WaPS economic dispatch is employed in [17], focusing on the network's supply side. Moazeni *et al.* [18] studied the economic dispatch of WaPS considering the energy management of various building applications. The demand response and frequency regulation of the water network are investigated in [19]. Zuloaga *et al.* [20] studied the operational resilience of WaPS under the condition of limited availability of water and/or energy. Focusing on the operation of WEN from the power system point of view, the utilization of energy flexibility through coordination of WaPS is investigated in [21]. Alhazmi *et al.* [22] studied the integration of WaPS using dc optimal power flow (DCOPF). Modeling such interconnected infrastructures individually is not preferred as it may result in suboptimal solutions in both networks. Joint operation of WaPS using a different power flow mechanism is investigated in [23]. The aforementioned studies investigated the operation of WaPS in different sectors under normal operating conditions in both networks, yet failed to study the operation of WaPS under emergency scenarios (i.e., failure in power transmission lines and/or in water network pipelines).

Mostly assuming "independent" network operation, the exiting studies on WaPS focus solely on the operation of one network alone and either entirely ignore or partially take into account a few of the other network's constraints [24]–[28]. The conventional models failed to comprehensively account for the "interdependent" operation of the integrated networks of

WaPS considering the complete operational constraints of both networks. The operation of WaPS faces growing challenges and vulnerability in the face of high impact low probability (HILP) events that cause damages to both networks, resulting in a partial or entire blackout in the systems. Lack of coordination between WaPS networks under emergency operating conditions may cause a delay in the recovery of both networks. Such lack of coordination was experienced during the hurricane Maria in Puerto Rico [29]. Hurricane Maria caused damage to nearly 90% of the power network in Puerto Rico, and various locations were not supplied with demanded water for a long time due to the severance of the hurricane and the absence of coordination between several interlinked sectors, e.g., power and water operators, which caused a delay in the response and recovery of both systems [30], [31].

Different from the state-of-the-art models, where the operation of WaPS is modeled and evaluated in normal operating conditions, this article bridges the gap in co-optimization and joint operation of WaPS under emergency scenarios. We propose a computationally efficient mixed-integer linear programming (MILP) formulation that jointly optimizes the operation of WaPS in presence of different contingencies in both power and water networks and under various disaster severity levels. Note that the disaster severity level is here reflected through the order of system contingencies (failures), i.e., the number of system elements failed or become unavailable. The presented model aims to enhance flexibility and advance the resilience of the joint WaPS in the face of infrastructure failures and extreme HILP events. Fig. 1 illustrates a big picture of the proposed framework for the integrated operation of the interdependent WaPS under emergency operating scenarios. First, the water and electricity data management system is formed by gathering the WaPS operation datasets. Then, if there is no damage observed in both power and water systems, the WaPS is concluded to be in the normal operating condition. However, if a failure in any component of the WaPS (either power or water networks or both) is realized, the proposed optimization under contingency will run to compute potential electric load outages. In summary, the main contributions of this article are as follows:

1) This article proposes a day-ahead optimization model for the operation of WaPS under emergency scenarios. The operational constraints of the water network are effectively modeled and integrated with the DCOPF models of the power system.
2) Different from the existing literature, the proposed model studies the contingencies in both power and water networks under various disaster severity levels, i.e., $N-1$, $N-2$, and $N-3$. The suggested model captures the contingencies in power generation units, transmission lines, and water network pumps.
3) The integrated model of WaPS include the complete hydraulic nonlinear constraints of the water network, and is thus nonlinear. The hydraulic constraints are linearized and the model gets transformed into a MILP formulation that can be effectively solved via the off-the-shelf solvers.

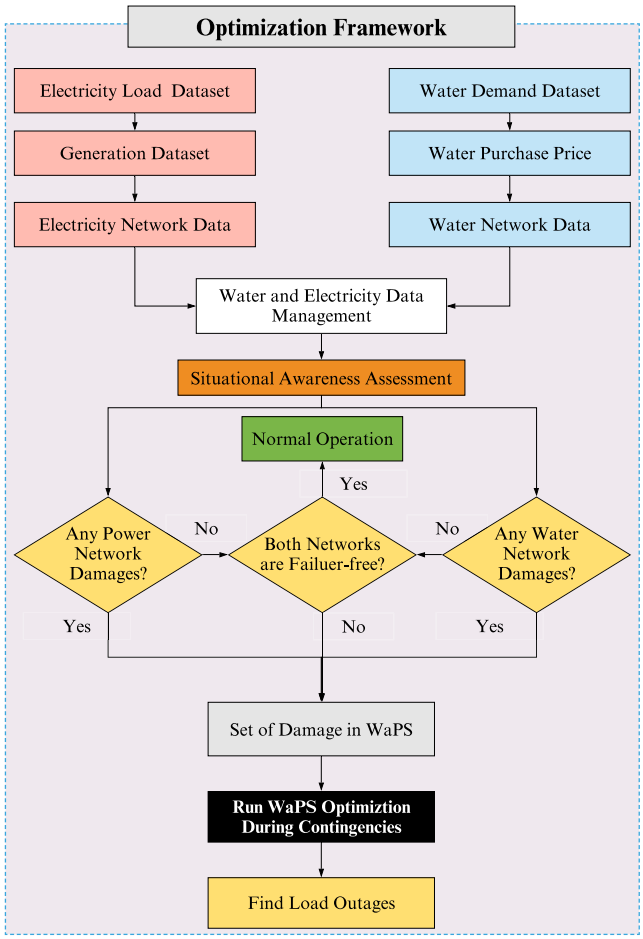

Fig. 1. Overview of the proposed methodology for optimal WaPS operation under emergency scenarios.

The rest of this article is organized as follows. Section II presents the proposed contingency-responsive joint optimization framework of power–water systems considering the complete hydraulic constraints of the water network. Numerical case studies and simulation results on a modified IEEE 24-bus reliability test system jointly operated with two and three 15-node water networks are presented in Section III. Finally, this article is concluded in Section IV.

II. Proposed Methodology

This section presents the proposed mathematical model for contingency analysis in a jointly operated WaPS. The proposed model of the water network consists of reservoirs, pipes, pumps, and tanks, which is mathematically represented using a directed graph $G=(\mathcal{N},\mathcal{A})$, where $\mathcal{N}$ denote the set of N water network nodes representing R reservoirs and T tanks. $\mathcal{A}$ is the set of A arcs, which consists of pipes and pumps. Water flow rate q is maintained by increasing the pressure head, using pump stations, or by adequate elevation difference between two nodes, such that if the water network is supplied by groundwater and the gravity is insufficient, a pumping station is needed to increase the pressure head and facilitate the flow of water. The water flow direction

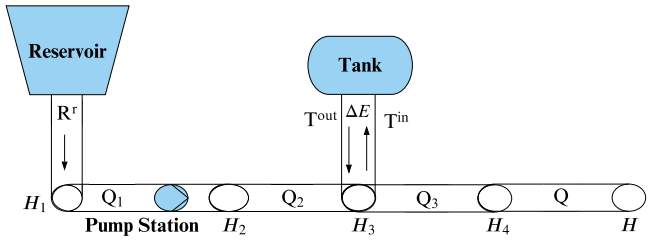

Fig. 2. Schematic diagram of the water network components.

is determined by the water flow rate's positive and negative values q. Water networks' schematic diagram and their hydraulic components are demonstrated in Fig. 2. Fig. 2 demonstrates the hydraulic components of a typical water network and shows the notations that are used in this article. The water moves from the reservoir R^r to customers through a network of water pipes. The water flow (Q) moves in the pipes by the pressure difference H or by increasing the pressure using pumps. Tank is used to store the water and assist the network during emergency operating conditions. ΔE_t denotes the difference between the tank water inflow (T^{in}) and outflow(T^{out}).

A. Objective Function

The WaPS operation objective during emergency operating conditions is to minimize the total cost of the system in the presence of contingencies. Therefore, the objective function is modeled by minimizing the cost of load outages and power generation in WaPS, formulated as follows:

$$\min \sum_{t=1}^{NT} \sum_{g=1}^{NG} \sum_{i=1}^{\mathcal{D}} \sum_{r=1}^{\mathcal{R}} \left(c_{i,t}^{sh} P_{i,t}^{sh} + c_{g,t} P_{g,t} + c_{r,t} R_t^r \right). \quad (1)$$

The proposed under-emergency optimization model is subjected to a set of constraints in both power and water networks described in the following.

B. WaPS Integration and Contingency Constraints

The contingencies in power systems are modeled within the DCOPF mechanism and is jointly formulated with the water network as follows:

$$P_{b,t}^{p,\text{adj}} = \sum_{p=1}^{P} \mathcal{C} P_t^p \qquad \forall b, \forall t \quad (2)$$

$$P_{\text{dn},t} = P_{d,t} + P_{b,t}^{p,\text{adj}} \qquad \forall n, \forall t \quad (3)$$

$$\underline{P_{\text{dn}}} \le P_{d,t} + P_{b,t}^{p,\text{adj}} \le \overline{P_{dn}} \qquad \forall n, \forall t \quad (4)$$

$$P_{k,t} = \frac{\theta_{n,t} - \theta_{m,t}}{x_k} \qquad \forall k, \forall t \quad (5)$$

$$-P_k^{\max} \nu_{k,t} \le P_{knm,t} \le P_k^{\max} \nu_{k,t} \qquad \forall k, \forall t \quad (6)$$

$$p_g^{\min} \phi_{g,t} \le P_{g,t} \le P_g^{\max} \phi_{g,t} \qquad \forall t \quad (7)$$

$$\sum_{g \in NG} P_{g,t} + \sum_{i \in \mathcal{D}} P_{i,t}^{\text{sh}} - \sum_{k \in L} P_{k,t} = \sum_{d \in D} P_{\text{dn},t} \qquad \forall t \quad (8)$$

$$0 \le P_{i,t}^{\text{sh}} \le P_{\text{dn},t} \qquad \forall i \in \mathcal{D}, n, \forall t. \quad (9)$$

Constraint (2) adjusts the dimension of pump electricity consumption, while constraint (3) integrates the water network's electricity consumption with power system demand. Total electricity demand for the joint WaPS is bounded in (4). The power flow in transmission lines is introduced in (5) and bounded to its maximum and minimum limits in (6), considering the availability status of lines $\nu_{k,t}$. Constraint (7) limits the output of each power generating unit to its maximum and minimum capacities, where $\phi_{g,t}$ identifies the status of generation units. Power balance constraint considering the load outage in WaPS is described in (8). The interrupted load is bounded above in (9) not to exceed the nodal load demand in normal operating conditions.

C. Water Flow Constraints

Water demand is delivered to customers through a network of pipes, pumps, and tanks. During peak hours, tanks are utilized to smoothen the pumpage demand to assist the water network during emergency scenarios. The water flow hydraulic constraints are modeled as follows:

$$R_t^r - D_t - Q_t - \Delta E_t = 0 \qquad \forall t \quad (10)$$

$$-Q_{\max} \le Q_t \le Q_{\max} \qquad \forall t \quad (11)$$

$$Q_t^p \ge 0 \qquad \forall t \quad (12)$$

$$H_{n,t} - H_{n+1,t} = r_p \mid Q_t^j \mid^{1.852} \text{Sign}(Q_t^j) \qquad \forall t \quad (13)$$

$$H_t^r - \hat{H} = 0 \qquad \forall t \quad (14)$$

$$H_{\min} \le H_t \le H_{\max} \qquad \forall t \quad (15)$$

$$V_{t+1} = V_t + \Delta E_t \qquad \forall t \quad (16)$$

$$\Delta E_t = T_t^{\text{in}} - T_t^{\text{out}} \qquad \forall t \quad (17)$$

$$\underline{\Delta E} \le \Delta E_t \le \overline{\Delta E} \qquad \forall t \quad (18)$$

$$V_t = S_a h_t \qquad \forall t \quad (19)$$

$$V_{\min} \le V_t \le V_{\max} \qquad \forall t \quad (20)$$

$$\Delta H_t = W_t \left(a_1 - a_2 \left(\frac{Q_t}{W_t} \right)^{a_3} \right) \qquad \forall t \quad (21)$$

$$P_t^p = W_t^3 \left(z_1 - z_2 \left(\frac{Q_t}{W_t} \right) \right) \qquad \forall t \quad (22)$$

$$P_{\min}^p \tau_t^p \le P_t^p \le P_{\max}^p \tau_t^p \qquad \forall p, \forall t. \quad (23)$$

The dynamic flow balance in the water network is formulated in (10). Water flow through pipelines and pumps are bounded in (11) and (12), respectively. The Hazen–Williams formula [32] is used in (13) to model the flow of water through pipes. Hazen–Williams formula is a quantitative term that is used to measure the pressure loss in water pipes due to friction. Constraints (14) set the pressure head at the reservoir node to

its geographical heights. Nodal pressure head is limited in (15). The dynamic operation of water flow in tanks is modeled in (16). Constraints (17) defines ΔE_t, which governs the difference between charging and discharging water flow of tanks. ΔE_t is limited in (18). Constraint (19) formulates the pressure head at the tank nodes, which is driven by the water stored in the related tanks. The volume of each tank is bounded in (20). Water pumps increase the nodal head pressure to increase the water flow. The controlled increase of pressure by pumps is formulated in (21). Pumps electricity consumption is modeled in (22). The availability status of water pump stations is bounded in (23).

D. Linearization

Nonlinearity is presented in constraints (13), (22), and (23). Solving nonlinear programming (NLP) models might be time-intensive, and an optimal feasible solution might not be guaranteed in large-scale water networks. Linearization and relaxation techniques are hence used to linearize and approximate the original NLP problem to a linear counterpart that is computationally more attractive and for which a globally optimal solution can be ensured. There are multiple techniques to linearize the nonlinear hydraulic constraints of a water network. A quasi-convex hull relaxation approach is used in [28] and [33] to relax the mixed-integer nonlinear programming (MINLP) models. Fooladivanda and Taylor [34] and Zamzam *et al.* [35] presented a mixed-integer second-order cone relaxation approach for finding the feasibility region of the water flow problem. Piece-wise linearization has been widely used in the literature to approximate the nonlinear functions of the hydraulic constraints [19], [21]–[23], [36], [37]. The convex piece-wise linearization has showed that the linear approximations of the hydraulic constraints can lead to a reasonably acceptable range of solutions in lower computation times; thus, due to the promising accuracy and computational benefits of the resulting linear optimization model, the piece-wise linearization technique was approached in this article to convert our NLP model to a MILP. The approximated linearized constraints are modeled as follows:

$$\sum_{i=1}^{I-1} Y_t^{i,j} = 1 \qquad \forall j, \forall t \quad (24)$$

$$X_t^{i,j} \le Y_t^{i-1,j} + Y_t^{i,j} \qquad \forall j, \forall i, \forall t \quad (25)$$

$$\sum_{i=1}^{I} X_t^{i,j} = 1 \qquad \forall j, \forall t \quad (26)$$

$$X_t^{I,j} \le Y_t^{I-1,j} \qquad \forall j, \forall t \quad (27)$$

$$X_t^{1,j} \le Y_t^{1,j} \qquad \forall j, \forall t \quad (28)$$

$$Q_t^j = \sum_{i=1}^{I} X_t^{i,j} q_i^j \qquad \forall j, \forall t \quad (29)$$

$$H_{n,t}^j - H_{n+1,t}^j = \sum_{i=1}^{I} X_t^{i,j} \Delta H_t^j(q_i^j) \qquad \forall j, \forall t \quad (30)$$

$$\sum_{u=1}^{U}\sum_{m=1}^{M} X_t^{u,m,p} = 1 \qquad \forall p, \forall t \quad (31)$$

$$Q_t^p = \sum_{u=1}^{U}\sum_{m=1}^{M} X_t^{u,m,p} q_u^p \qquad \forall p, \forall t \quad (32)$$

$$W_t = \sum_{u=1}^{U}\sum_{m=1}^{M} X_t^{u,m,p} w_m^p \qquad \forall p, \forall t \quad (33)$$

$$\Delta H_t^p = \sum_{u=1}^{U}\sum_{m=1}^{M} \Delta H_t^p(q_u^p, w_m^p) X_t^{u,m,p} \qquad \forall p, \forall t \quad (34)$$

$$P_t^p = \sum_{u=1}^{U}\sum_{m=1}^{M} P_t^p(q_u^p, w_m^p) X_t^{u,m,p} \qquad \forall p, \forall t \quad (35)$$

$$\sum_{u=1}^{U}\sum_{m=1}^{M} \left(H_{u,m,p,t}^{\text{Upper}} + H_{u,m,p,t}^{\text{Lower}}\right) = 1 \qquad \forall p, \forall t \quad (36)$$

$$X_t^{u,m,p} \le H_{u,m-1,p,t}^{\text{Upper}} + H_{u+1,m,p,t}^{\text{Upper}} + H_{u,m,p,t}^{\text{Upper}} + H_{u-1,m,p,t}^{\text{Lower}} + H_{u,m+1,p,t}^{\text{Lower}} + H_{u,m,p,t}^{\text{Lower}} \qquad \forall u, \forall m, \forall p, \forall t \quad (37)$$

Constraints (24)–(30) represent the linear approximation for the nonlinear constraint (13). Constraints (24) drives only one binary variable to take the value of 1, while (25)–(28) indicate that only nonzero values are selected for $X_t^{i,j}$ and $X_t^{i+1,j}$. Pressure head difference for pipes is ensured to be selected appropriately to evaluate the approximated functions in constraints (29)–(30). The linearized formulation of the nonlinear constraints (21)–(22) is modeled using the triangle technique in (31)–(37). Constraint (31) presents the weight of the convex combination of the selected triangle. The linear combinations of any selected values for water flow through pumps and pump's speed are modeled in (32) and (33), respectively, while the bivariate nonlinear functions for each pump's pressure difference and electricity consumption are approximated in (34) and (35), respectively. Only one triangle is forced to be selected in constraint (36) for the convex combination, and constraint (37) ensures that only values other than zero of $X_t^{i,m,p}$ can be associated with all three vertices of the triangle. Detailed illustration of the linearization technique is provided in [23].

The complete formulation for the integrated WaPS in the form of a MILP optimization model is presented in the following, which considers the contingency-driven emergency response in the joint operation of WaPS.

$$\min(1)$$

$$\text{subject to } (2)-(12), (14)-(20), (23)-(37)$$

III. Numerical Case Studies

A. System Descriptions, Data, and Assumptions

The proposed formulation for the resilient operation of the interconnected power and water networks under contingency scenarios is applied on a modified IEEE 24-bus reliability test

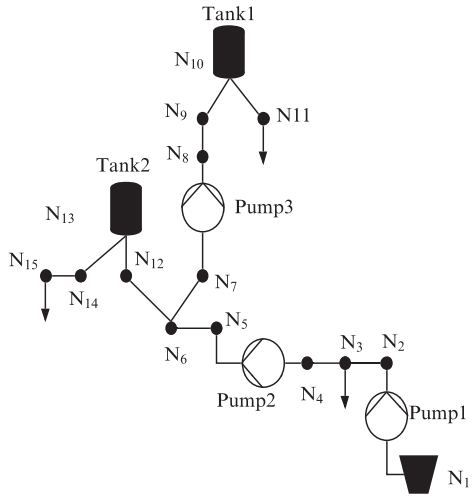

Fig. 3. Schematic diagram of the commercial-scale 15-node water network.

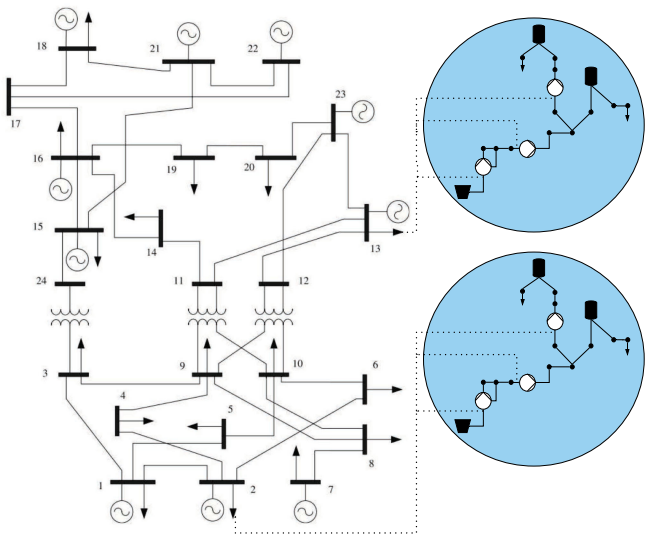

Fig. 4. Schematic diagram of the IEEE 24-bus reliability test system supplying two water networks.

system jointly operated and connected to two commercial-scale water networks. The IEEE 24-bus reliability test system consists of 12 generating units, 34 transmission lines, and 17 load points. Each water network consists of 15 nodes connected to a power grid load point, as shown in Fig. 4. Each water network consists of 15 nodes, i.e., 11 pipelines, 3 pumps, and 2 tanks, and is connected to a power grid load point. The precise locations for each water network component, e.g., pumping stations, water tanks, water demand nodes, etc., are illustrated in Fig. 3. The initial volume of all water tanks is set to zero. All data for the studied WaPS (i.e., generation capacity, load profiles, transmission line parameters, water demand profiles, pipeline parameters, etc.) are provided in [38] and [39]. The simulations are performed using CPLEX solver to handle the reformulated MILP model. A mathematical programming language (AMPL) environment [40], using a PC with an Intel Xeon E5-2620 v2 processor, 16 GB of memory, and 64-bit operating system, is used to perform all the simulations.

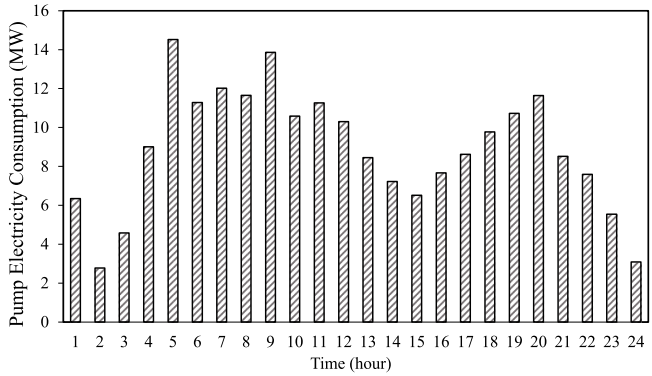

Fig. 5. Scheduled electricity consumption of water pumps in normal operating condition: CS-I.

B. Results and Discussions

In order to demonstrate the performance of the proposed model, four different case studies are presented:

1) *Case Study I (CS-I)* presents the *day-ahead normal operation* of the WaPS, which integrates water networks' and the power network's operations jointly and interdependently, where the DCOPF mechanism and hydraulic water constraints are efficiently integrated.
2) *Case Study II (CS-II)* models the $N-1$ contingencies in the joint operation of the WaPS, taking into account the DCOPF mechanism for the power network and water network hydraulic model in emergency states.
3) *Case Study III (CS-III)* represents the joint operation of the WaPS under a higher (e.g., level-2) disaster severity, i.e., $N-2$ contingencies, taking into account simultaneous failures in two components of the WaPS, thereby emergency operation of WaPS.
4) *Case Study IV (CS-IV)* represents the operation of the WaPS under a higher disaster severity, i.e., $N-3$ contingencies.

Fig. 5 illustrates the day-ahead electricity consumption of water pumps in *CS-I*, when the joint WaPS operates normally. Water tanks' performance for the 24-h operation period is shown in Fig. 6. It can be observed from Fig. 6 that water tanks are assisting the water network during peak hours (e.g., hours 7–13) by discharging (negative value) and supplying the water demand, while it is charging (positive value) during off-peak hours (e.g., hours 1–7). The daily load profile for the integrated WaPS in *CS-I* is shown in Fig. 7. In the face of emergencies, i.e., *CS-II*, *CS-III* and *CS-IV*, the amount of load shad at each hour is evaluated as demonstrated in Fig. 8.

The operational cost for all case studies and the computational results are presented in Table I. The total operating cost for *CS-I*, when normal operation of the joint WaPS is studied, is reported at \$42 348.17. The optimal operation cost for the interlinked WaPS, taking into account the failure of one component of the WaPS (i.e., $N-1$ scenarios) in *CS-II* and two components

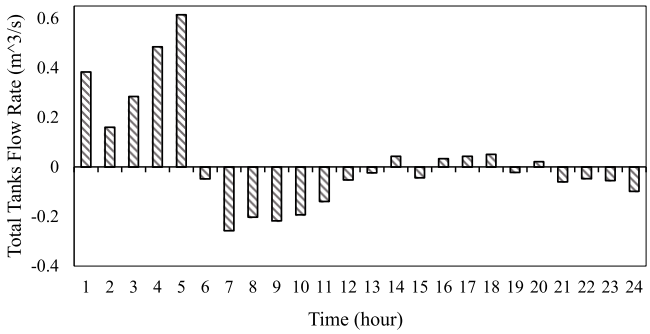

Fig. 6. Scheduled water flow rate of tanks in normal operating conditions: CS-I.

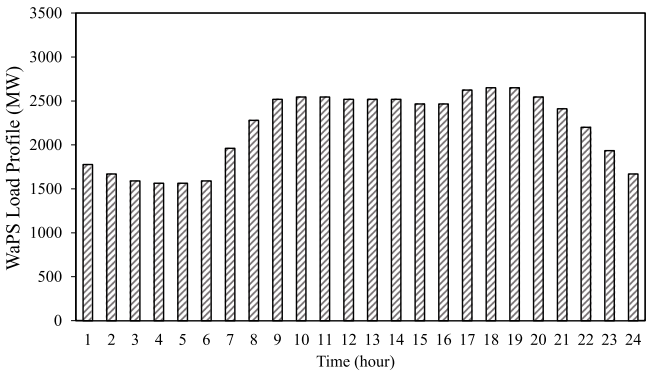

Fig. 7. Load Profile for the integrated WaPS in normal operating conditions: **CS-I**.

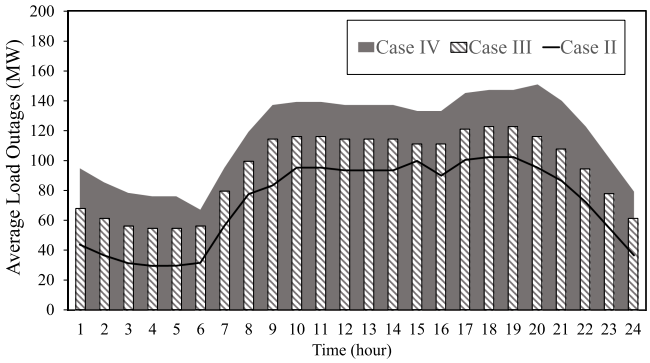

Fig. 8. Average load outage in WaPS when contingencies are applied.

(i.e., $N-2$ scenarios) in *CS-III*, are recorded at \$45 113.22 and \$47 234.72, respectively. In *CS-IV* with $N-3$ contingency analysis, the operation cost of the joint WaPS is reported at \$50 027.92. As expected, one can observe that the higher the number of contingencies, the higher the WaPS operation cost.

The computation time for *CS-I* is reported 92.1 s, while that of the *CS-II* and *CS-III* are recorded at 123.2 s and 149.2 s, respectively. The computation time for *CS-IV* is noted 164.3 s. It can be observed that the proposed solution is computationally efficient to be used for the integrated operation of WaPS under emergencies.

TABLE I
TOTAL OPERATION COST AND OPTIMIZATION COMPUTATION TIME IN DIFFERENT TEST CASES

Case #	Operation Cost (\$)	Time (s)
CS-I	42,348.17	92.1
CS-II	45,113.22	123.2
CS-III	47,234.72	149.2
CS-IV	50,027.92	164.3

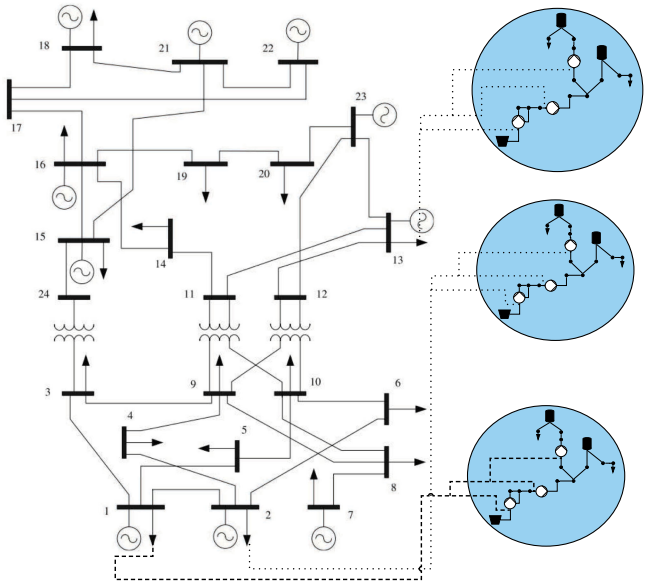

Fig. 9. Schematic diagram of the IEEE 24-bus reliability test system supplying three water networks.

TABLE II
TOTAL OPERATION COST AND OPTIMIZATION COMPUTATION TIME IN DIFFERENT CONTINGENCY SCENARIOS

Scenario #	Operation Cost (\$)	Time (s)
$N-1$	56,245.05	112.4
$N-2$	59,950.23	153.6
$N-3$	61,412.95	170.9

C. On the Scalability of the Proposed Framework: Impact of an Additional Water Network

In order to evaluate the effectiveness and the scalability of the proposed framework, we study the impact of adding an additional water network to the integrated system. A total of three water networks are jointly operated with the IEEE 24-bus reliability test system. Fig. 9 shows a schematic diagram of the studied system. Water networks are connected to load points 1, 2, and 13. The new model is tested under three contingency scenarios, i.e., $N-1$, $N-2$, and $N-3$. The operational cost for all contingency scenarios and the computational results are shown in Table II. Under $N-1$ scenario, when one network component fails, the total outage cost is computed as \$56 245.05. The computational time is recorded at 112.4 s. When $N-2$ and $N-3$ contingency scenarios are applied to the integrated WaPS model, the total cost of outages is reported at \$59 950.23 and \$61 412.95, respectively. During such emergency conditions, the amount of load shad at each hour is demonstrated in Fig. 10.

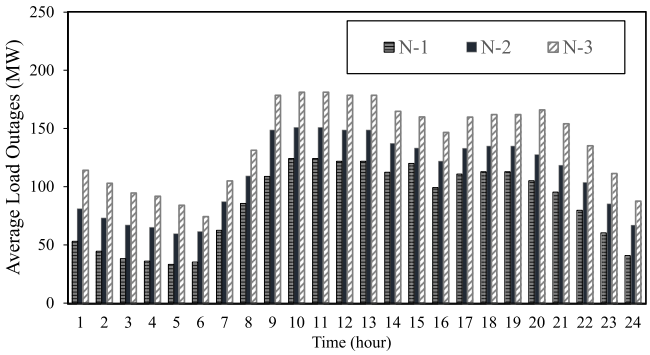

Fig. 10. Average load outage in WaPS when contingencies are applied.

The computational time when $N-2$ and $N-3$ scenarios are applied is found at 153.6 s and 170.9 s, respectively. The numerical results demonstrate that the proposed framework is scalable and the computational time is acceptable for decision-making on the daily operation of the interconnected networks.

IV. Conclusion

Different from the state-of-the-art models, this article proposed a novel framework for the joint and coordinated operation of the water and electricity networks under contingency scenarios. In order to comprehensively evaluate the effectiveness of the interconnected WaPS, the DCOPF mechanism and hydraulic water system operation have been taken into account. Piece-wise linearization technique was used to approximate the hydraulic water constraints and convert the NLP model to a tractable MILP formulation, which commercial off-the-shelf solvers can quickly solve. The proposed model was applied to IEEE 24-bus reliability power test system connected to two commercial-scale water networks, each consisting of 15 nodes. To further verify the efficiency and scalability of the proposed framework on large-scale systems, the proposed model was applied to a higher number of water networks, i.e., three water networks, each consisting of 15 nodes supplied by the IEEE 24-bus power test system. The simulation results included $N-1$, $N-2$, and $N-3$ contingency scenarios and demonstrated the promising performance of the proposed integrated WaPS model in enhancing the reliability and resilience of the critical WaPS infrastructures during failure emergencies.

References

[1] V. M. Leiby and M. E. Burke, *Energy Efficiency Best Practices for North American Drinking Water Utilities*. Denver, CO, USA: Water Res. Found., 2011.

[2] B. Appelbaum, "Water & sustainability: US electricity consumption for water supply & treatment-the next half century," *Elect. Power Res. Inst.*, Palo Alto, CA, USA, vol. 4, Rep. 1006787, 2002.

[3] C. Copeland, "Energy-water nexus: The water sector's energy use," Congressional Res. Service, Washington, DC, USA, Rep. R43199, Jan. 2014.

[4] G. Klein, M. Krebs, V. Hall, T. O'Brien, and B. Blevins, "California's water-energy relationship," *California Energy Commission*, Sacramento, CA, USA, Rep. CEC-700-2005-011-SF, 2005.

[5] S. Shin *et al.*, "A systematic review of quantitative resilience measures for water infrastructure systems," *Water*, vol. 10, no. 2, 2018, Art. no. 164, doi: 10.3390/w10020164.

[6] X. Zhang and V. V. Vesselinov, "Energy-water nexus: Balancing the tradeoffs between two-level decision makers," *Appl. Energy*, vol. 183, pp. 77–87, 2016.

[7] Q. Li, S. Yu, A. Al-Sumaiti, and K. Turitsyn, "Modeling and Co-Optimization of a Micro Water-Energy Nexus for Smart Communities," *2018 IEEE PES Innovative Smart Grid Technol. Conf. Europe (ISGT-Europe)*, 2018, pp. 1–5, doi: 10.1109/ISGTEurope.2018.8571840.

[8] A. Santhosh, A. M. Farid, and K. Youcef-Toumi, "Optimal network flow for the supply side of the energy-water nexus," in *Proc. IEEE Int. Workshop Intelli. Energy Syst.*, 2013, pp. 155–160.

[9] C. A. Scott, S. A. Pierce, M. J. Pasqualetti, A. L. Jones, B. E. Montz, and J. H. Hoover, "Policy and institutional dimensions of the water-energy nexus," *Energy Policy*, vol. 39, no. 10, pp. 6622–6630, 2011.

[10] C. Ringler, A. Bhaduri, and R. Lawford, "The nexus across water, energy, land and food (WELF): Potential for improved resource use efficiency?," *Curr. Opin. Environ. Sustainability*, vol. 5, no. 6, pp. 617–624, 2013.

[11] U. Lele, M. Klousia-Marquis, and S. Goswami, "Good governance for food, water and energy security," *Aquatic Procedia*, vol. 1, pp. 44–63, 2013.

[12] S.-C. Kao *et al.*, "Projecting changes in annual hydropower generation using regional runoff data: An assessment of the United States federal hydropower plants," *Energy*, vol. 80, pp. 239–250, 2015.

[13] N. Vakilifard, M. Anda, P. A. Bahri, and G. Ho, "The role of water-energy nexus in optimising water supply systems-review of techniques and approaches," *Renewable Sustain. Energy Rev.*, vol. 82, pp. 1424–1432, 2018.

[14] W. N. Lubega and A. M. Farid, "Quantitative engineering systems modeling and analysis of the energy-water nexus," *Appl. Energy*, vol. 135, pp. 142–157, 2014.

[15] D. Fang and B. Chen, "Linkage analysis for the water-energy nexus of city," *Appl. Energy*, vol. 189, pp. 770–779, 2017.

[16] A. Santhosh, A. M. Farid, and K. Youcef-Toumi, "The impact of storage facility capacity and ramping capabilities on the supply side economic dispatch of the energy-water nexus," *Energy*, vol. 66, pp. 363–377, 2014.

[17] A. Santhosh, A. M. Farid, and K. Youcef-Toumi, "Real-time economic dispatch for the supply side of the energy-water nexus," *Appl. Energy*, vol. 122, pp. 42–52, 2014.

[18] F. Moazeni, J. Khazaei, and A. Asrari, "Step towards energy-water smart microgrids; buildings thermal energy and water demand management embedded in economic dispatch," *IEEE Trans. Smart Grid*, vol. 12, no. 5, pp. 3680–3691, Sep. 2021.

[19] K. Oikonomou, M. Parvania, and R. Khatami, "Optimal demand response scheduling for water distribution systems," *IEEE Trans. Ind. Inform.*, vol. 14, no. 11, pp. 5112–5122, Nov. 2018.

[20] S. Zuloaga, P. Khatavkar, L. Mays, and V. Vittal, "Resilience of cyber-enabled electrical energy and water distribution systems considering infrastructural robustness under conditions of limited water and/or energy availability," *IEEE Trans. Eng. Manage.*, vol. 69, no. 3, pp. 639–655, Jun. 2022.

[21] K. Oikonomou and M. Parvania, "Optimal coordination of water distribution energy flexibility with power systems operation," *IEEE Trans. Smart Grid*, vol. 10, no. 1, pp. 1101–1110, Jan. 2019.

[22] M. Alhazmi, P. Dehghanian, M. Nazemi, and M. Mitolo, "Joint operation optimization of the interdependent water and electricity networks," in *Proc. IEEE Ind. Appl. Soc. Annu. Meeting*, 2020, pp. 1–7.

[23] M. Alhazmi and P. Dehghanian, "Optimal integration of interconnected water and electricity networks," *IET Gener. Transmiss. Distrib.*, vol. 15, pp. 2033–2043, 2021.

[24] A. Stuhlmacher and J. L. Mathieu, "Chance-constrained water pumping managing power distribution network constraints," in *Proc. IEEE North Amer. Power Symp.*, 2019, pp. 1–6.

[25] H. Han, K. Oikonomou, N. Chalapathi, M. Parvania, and B. Wang, "Interactive visualization of interdependent power and water infrastructure operation," in *Proc. IEEE Power Energy Soc. Innov. Smart Grid Technol. Conf.*, 2020, pp. 1–5.

[26] K. Oikonomou and M. Parvania, "Optimal coordinated operation of interdependent power and water distribution systems," *IEEE Trans. Smart Grid*, vol. 11, no. 6, pp. 4784–4794, Nov. 2020.

[27] Q. Li, S. Yu, A. Al-Sumaiti, and K. Turitsyn, "Modeling and co-optimization of a micro water-energy nexus for smart communities," in *Proc. IEEE PES Innov. Smart Grid Technol. Conf. Europe*, 2018, pp. 1–5.

[28] A. Stuhlmacher and J. L. Mathieu, "Chance-constrained water pumping to manage water and power demand uncertainty in distribution networks," *Proc. IEEE*, vol. 108, no. 9, pp. 1640–1655, Sep. 2020.

[29] P. Brown *et al.*, "Hurricanes and the environmental justice island: Irma and maria in Puerto Rico," *Environ. Justice*, vol. 11, no. 4, pp. 148–153, 2018.
[30] R. Subramanian *et al.*, "Air quality in Puerto Rico in the aftermath of hurricane maria: A case study on the use of lower cost air quality monitors," *ACS Earth Space Chem.*, vol. 2, no. 11, pp. 1179–1186, 2018.
[31] Y. Lin *et al.*, "Impact of hurricane maria on drinking water quality in Puerto Rico," *Environ. Sci. Technol.*, vol. 54, no. 15, pp. 9495–9509, 2020.
[32] L. W. Mays, *Water Resources Engineering*. Hoboken, NJ, USA: Wiley, 2010.
[33] Q. Li, S. Yu, A. S. Al-Sumaiti, and K. Turitsyn, "Micro water-energy nexus: Optimal demand-side management and quasi-convex hull relaxation," *IEEE Trans. Control Netw. Syst.*, vol. 6, no. 4, pp. 1313–1322, Dec. 2019.
[34] D. Fooladivanda and J. A. Taylor, "Energy-optimal pump scheduling and water flow," *IEEE Trans. Control Netw. Syst.*, vol. 5, no. 3, pp. 1016–1026, Sep. 2018.
[35] A. S. Zamzam, E. Dall'Anese, C. Zhao, J. A. Taylor, and N. D. Sidiropoulos, "Optimal water-power flow-problem: Formulation and distributed optimal solution," *IEEE Trans. Control Netw. Syst.*, vol. 6, no. 1, pp. 37–47, Mar. 2019.
[36] K. Oikonomou, M. Parvania, and S. Burian, "Integrating water distribution energy flexibility in power systems operation," in *Proc. IEEE Power Energy Soc. Gen. Meeting*, 2017, pp. 1–5.
[37] K. Oikonomou and M. Parvania, "Optimal participation of water desalination plants in electricity demand response and regulation markets," *IEEE Syst. J.*, vol. 14, no. 3, pp. 3729–3739, Sep. 2020.
[38] "Water network data information," Accessed: Mar. 30, 2022. [Online]. Available: https://drive.google.com/file/d/1f-O22eKI2LMSKdZPquOaRw8kbqeczCEv/view
[39] "IEEE 24-bus RTS data information," Accessed: Mar. 30, 2022. [Online]. Available: https://backend.orbit.dtu.dk/ws/portalfiles/portal/120568114/An_Updated_Version_of_the_IEEE_RTS_24Bus_System_for_Electricty_Market_an....pdf
[40] R. Fourer, D. M. Gay, and B. W. Kernighan, "AMPL: A modeling language for mathematical programming," Thomson, 2003.
[41] M. Alhazmi, P. Dehghanian, M. Nazemi, F. Wang, and A. Alfadda, "Coordination framework for integrated operation of water-power systems under contingencies," in *Proc. IEEE Ind. Appl. Soc. Annu. Meeting*, 2021, pp. 1–7.

Mohannad Alhazmi (Student Member, IEEE) received the B.Sc. and M.Sc. degrees in electrical engineering from Umm Al-Qura University, Saudi Arabia, in 2013, and The George Washington University, Washington D.C., USA, in 2017, respectively. He is currently working toward the Ph.D. degree with the Department of Electrical and Computer Engineering, The George Washington University.

He is currently with the Electrical Engineering Department, College of Engineering, King Saud University, Riyadh, Saudi Arabia. His research interests include power system reliability and resiliency as well as operation of interdependent critical infrastructures.

Payman Dehghanian (Senior Member, IEEE) received the B.Sc. degree in electrical engineering from University of Tehran, Tehran, Iran, in 2009, the M.Sc. degree in electrical engineering from Sharif University of Technology, Tehran, Iran, in 2011, and the Ph.D. degree, in electrical engineering from Texas A&M University, Texas, USA, in 2017.

He is currently an Assistant Professor with the Department of Electrical and Computer Engineering in George Washington University, Washington, D.C., USA. His research interests include power system protection and control, power system reliability and resiliency, asset management, and smart electricity grid applications.

Dr. Dehghanian is the recipient of the 2014 and 2015 IEEE Region 5 Outstanding Professional Achievement Awards, the 2015 IEEE-HKN Outstanding Young Professional Award, and the 2021 Early Career Award from the Washington Academy of Sciences.

Mostafa Nazemi (Student Member, IEEE) received the B.Sc. degree in electrical engineering from the K. N. Toosi University of Technology, Tehran, Iran, in 2015, and the M.Sc. degree in energy systems engineering from the Sharif University of Technology, Tehran, Iran, in 2017. He is currently working toward the Ph.D. degree in electrical engineering with the Department of Electrical and Computer Engineering, George Washington University, Washington, DC, USA.

His research interests include power system resilience, power system planning and operation, energy optimizations, and smart electricity grid applications.

Mr. Nazemi was the recipient of the 2018 Certificate of Excellence in Reviewing by the Editorial Board Committee of the *Journal of Modern Power and Clean Energy* for his contributions to the journal.

Fei Wang (Senior Member, IEEE) received the B.S. degree in electrical engineering from Hebei University, Baoding, Baoding, China, in 1993, the M.S. and Ph.D. degrees in electrical engineering from North China Electric Power University (NCEPU), Baoding, China, in 2005 and 2013, respectively.

He is currently a Professor with the Department of Electrical Engineering, NCEPU and the State Key Laboratory of Alternate Electrical Power System with Renewable Energy Sources, Baoding and Beijing, China. He is the Director of Smart Energy Network Integrated Operation Research Center (SENIOR) and the Leader of "Double First-Class" research team project at NCEPU. He was a Visiting Professor with the Department of Electrical and Computer Engineering, University of Illinois at Urbana-Champaign, Urbana, IL, USA, from 2016 to 2017. He was a Researcher with the Department of Electrical Engineering, Tsinghua University, Beijing, China, from 2014 to 2016. His research interests include renewable energy power, electricity price and electricity load forecasting, demand response and electricity market, smart grid, microgrid and integrated energy system.

Abdullah Alfadda received the B.Sc. degree in electrical engineering from King Saud University, Riyadh, Saudi Arabia, in 2009, the M.Sc. degree in electrical engineering from Virginia Tech, Blacksburg, VA, USA, in 2015, and the Ph.D. degree in computer engineering from Virginia Tech, Blacksburg, VA, USA, in 2019. He is currently an Assistant Research Professor with King Abdulaziz City for Science and Technology, Riyadh, Saudi Arabia. His research interests include forecasting and AI models for renewable energy resources, solar and storage integration, tariff design, electricity consumers' behavior.